RSC Advances

RSC Advances

www.rsc.org/advances

Journal Name

ARTICLE

Sensitive and selective amplified detection of silver ion based on NEase-aided target recycling

Kai Zhang,[*] Ke Wang, Xue Zhu, and Minhao Xie

G-quadruplex-hemin complexes are DNAzyme peroxidases that efficiently catalyze H_2O_2-mediated reactions, such as the oxidation of $ABTS^{2-}$ (2,2′-azinobis(3-ethylbenzothiozoline)-6-sulfonate) by H_2O_2. On the other hand, nicking endonucleases are a special family of restriction endonucleases that can recognize a specific sequence of a double-stranded DNA (dsDNA) and cut one strand of this dsDNA. This function has been used to develop different nicking enzyme based amplified detection platforms for biosensing of different analytes. On the basis of this principle, a highly sensitive and selective Ag^+-detection strategy was developed in this work. The strategy mainly consists of DNA1, DNA2, and DNA3. DNA1 includes two G-riched DNAzyme segments, the recognition sequence and cleavage site for nicking endonuclease (NEase), and the hybridization part for DNA2. DNA2 is designed to be partly complementary to both ends of DNA1. DNA3 is designed to be complementary to DNA1 with one mismatched cytosine-cytosine. The hybridization of DNA1 and DNA2 results in DNA1 forming a closed structure. Upon addition of Ag^+, DNA1 can be cleaved into pieces by this NEase, which leads to the denaturation of the DNA1/DNA2/DNA3 complex. Therefore, segments of DNA1 folds into G-quadruplex, which is able to effectively catalyze the H_2O_2-mediated oxidation of $ABTS^{2-}$ in the presence of hemin, producing the free-radical ion $ABTS^{\cdot-}$, which has a maximal absorption at 418 nm. The method allows simple detection of Ag^+ with a detection limit of 0.01 nM. As a strong Ag^+-binder, this Ag^+-sensing system was also developed as a Cys-sensing system.

Introduction

Silver ion (Ag^+), one of the most hazardous pollutants, is always unrestrictedly released into the environment from industrial wastes. Also, Ag^+ has serious biological effects on human health. Exposure to Ag^+ may lead to argyria and severe symptoms such as headache, stomach distress, organ edema, skin irritation, and even death.[1, 2] Therefore, accurate detection of trace Ag^+ is of great importance and has become a hot topic in scientific research. On account of the significance of Ag^+, the assays of Ag^+ have received more and more interest, and various techniques have been employed including surface plasmon resonance (SPR),[3] colorimetric assay,[4] etc. However, most of the methods are time consuming or not sensitive enough. These disadvantages restrict further development of heavy metal ion sensors. In addition, several methods have been developed for the assay of Ag^+ based on organic fluorophores or semiconductor quantum dots, and an Ag^+-selective electrode with a high limit of detection was realized.[5-7] However, these technologies always require the use of labelled fluorophores (donors) and quenchers (acceptors) for tagging, and quantum dots (QDs) or nanoparticles, which inevitably results in complicated or expensive operation. Thus, a new method with high sensitivity and selectivity for the detection of silver ions is needed. On the other hand, DNA–metal base pairs attract considerable attention because of their potential in sensing applications.[8] Some metal ions can selectively bind to a few native or artificial bases in DNA duplexes to form metal-mediated base pairs.[8-10] This general property gives rise to an increase in the thermal stability of DNA duplexes. Especially,

DNA–metal base pairs are often utilized to promote a structural change in single- or double-stranded oligonucleotides, which enables the detection of metal ions (e.g., Hg^{2+} and Ag^+) by various means. [9, 10] Cytosine–cytosine (C–C) pairs in DNA duplexes are able to exclusively capture Ag^+ to form $C–Ag^+–C$ base pairs. [1, 11] Based on this feature, many DNA-based fluorescent Ag^+ sensors have been constructed. However, most of these proposed strategies also suffer from the limitations as "signal-off" architectures. [4] Such "signal-off" assays might show lower sensitivity than "turn-on" methods and may repot false positive results caused by other quenchers or environmental stimulus in real samples, which are undesirable for practically analytical applications.[12] Therefore, it is highly desirable to design label-free and "signal-on" method for the detection of Ag^+.

On the other hand, G-quadruplexes are unique higher-order structures in which G-rich nucleic acid sequences form stacked arrays of G-quartets connected by Hoogsteen-type base pairing. [13, 14] Sequences with the potential to form G-quadruplex structures are common in biologically important chromosomal features such as telomeres, gene promoters, and immunoglobulin switch regions, so they have become an important research focus. The discovery that some G-quadruplex-hemin complexes have peroxidase-like activity was an important step in the investigation of these structures.[15, 16] This class of peroxidase-like G-quadruplex-hemin DNAzyme has been used to detect telomerase activity,[17] small molecules and metal ions,[18] to screen G-quadruplex ligands and to develop DNA sensors.[13]

Nicking endonucleases are a special family of restriction endonucleases that can recognize a specific sequence of a double-stranded DNA (dsDNA) and cut one strand of this dsDNA.[8] This function has been used to develop different nicking enzyme based amplified detection platforms for biosensing of different analytes.[8] Some techniques based on nicking enzyme are demonstrated for development of homogeneous fluorescence or colorimetric aptasensors.[19] However, most of the current nicking enzyme based optical aptasensors require the additional modification of aptamer probes or signaling DNA probes.

Enlightened by the above facts, we envision that a new Ag^+ detection strategy can be devised utilizing the advantages of both the nicking endonuclease-assisted signaling amplification (NEASA) strategy and the label-free architecture of G-quadruplex-hemin complex. This method does not need any chemical modification of DNA probe for labeling; the target molecule can be simply detected with UV-vis absorbance spectroscopy, which makes it a simple and cost-effective method. For the detection of Ag^+, this sensing platform exhibited high sensitivity and specificity. The proposed sensing platform promises a powerful approach for amplified analysis of target molecules.

Experimental

Materials and chemicals

The oligouncleotides were purchased from Genscript Biotechnology Co., Ltd (Nanjing, China) and their sequences were listed in Table 1. H_2O_2, 2,2′-azinobis(3-ethylbenzothiozoline)-6-sulfonate ($ABTS^{2-}$), hemin, amino acids and the used metal salts ($AgNO_3$, $Mg(NO_3)_2$, $Cu(NO_3)_2$,

$Mn(Ac)_2$, $Zn(Ac)_2$, $Pb(NO_3)_2$, $Ni(NO_3)_2$, $Cd(NO_3)_2$, $Fe(NO_3)_3$, $Hg(Ac)_2$, and $Ca(Ac)_2$) were obtained from Sigma. All chemical reagents were of analytical grade and used without further purification.

Three strands of oligonucleotides were adopted in our experiments. The sequences are as flows: DNA1, **5'-CAC AGG GTT GGG CGG GAT GGG TGC TGG GTG ACT** *TCT CCA TCC AT* **CTG GGG TAG GGC GGG TTG GGA ATT-3'**, DNA2, 5'-CCC TTA AGT GTC CC-3', and DNA3: 5'-*ATG GAT GGA CA*-3'. DNA1 contains three functional regions: the sequence shown in bold are G-riched DNAzyme segments; (2) the underlined sequence can complement to the underlined sequence of DNA2; (3) the italic sequence is a linker complementary to the DNA3 at the help of Ag^+.

2.2 Gel electrophoresis

Nondenaturing polyacrylamide gel electrophoresis (PAGE) (20%) was carried out in 1× TBE buffer at a 120 V constant voltage for 1.5 h at room temperature. Before amplification reaction, the mixture of DNA1 and DNA2 was heated to 90 °C for 10 min and allowed to cool to room temperature for about 4 h to form the partially complementary dsDNA. Then, the above solution was incubated in Nt.CviPII solution (0.5 U/μL) containing 4 μM DNA3 and 100 nM Ag^+ at 37 °C for 1 h. Afterward, digestions were stopped by heating at 90 °C for 10 min. The gel was taken photograph under UV light after staining with EtBr for 15 min. The concentration of each DNA is 1 μM.

Ag^+ detection

The DNA1 and DNA2 solution (3 μM each) was prepared in 10 mM Tris-HAc buffer (pH = 7.0) containing 1 mM MgAc. The above solution was heated to 90 °C for 10 min, and then cooled slowly to room temperature for about 4 h. Different concentrations of Ag^+ were added, and the solutions were incubated at 37 °C for 15 min to make the DNA2 contact with the Ag+ completely. To each solution was added 1.2 μM DNA3, then, the mixture was allowed to incubate at 37 °C for another 45 min. Afterward, digestions were stopped by heating at 90 °C for 10 min. 1 μM of hemin in Tris-HAc buffer (contain 10 mM KNO_3) was added to the mixture and the mixture was held for 1 h. Then, 3.0 mM of $ABTS^{2-}$ and 2.0 mM of H_2O_2 were added. The absorption spectrum of the reaction product $ABTS^{-}$ was recorded using a TU-1901UV-Vis spectrophotometer after the reaction had run for 5 min. The absorbance at 418 nm was used for quantitative analysis. For real samples analysis, different concentrations of Ag^+ were detected in drinking water and lake water.

In order to achieve optimal assay conditions, the K^+ concentrations were optimized. As displayed in Fig.S1, the absorbance of the solution increases rapidly with increasing the concentration of K^+ in the range from 0 to 10 mM and reaches a plateau thereafter. To ensure complete reactions, the 10 mM was selected for subsequent experiments.

Cys detection

The DNA1 and DNA2 solution (3 μM each) was prepared in 10 mM Tris-HAc buffer (pH = 7.0) containing 1 mM MgAc. The DNA solution was heated to 90 °C for 10 min, and then

cooled slowly to room temperature for about 4 h. 100 nM Ag^+ was added and the solution was incubated at 37 °C for 15 min. To this solution was added 1.2 μM DNA3, the mixture was allowed to incubate at 37 °C for 15 min. Then, different concentrations of Cys were added, and each mixture was incubated at 37 °C for another 30 min. Afterward, digestions were stopped by heating at 90 °C for 10 min. 1 μM of hemin was added to the mixture and the mixture was held for 1 h. Then, 3.0 mM of $ABTS^{2-}$ and 2.0 mM of H_2O_2 were added. The absorption spectrum of the reaction product $ABTS^{·-}$ was recorded using a TU-1901 UV-Vis spectrophotometer after the reaction had run for 5 min. The absorbance at 418 nm was used for quantitative analysis

Results and discussion

Mechanism of this strategy
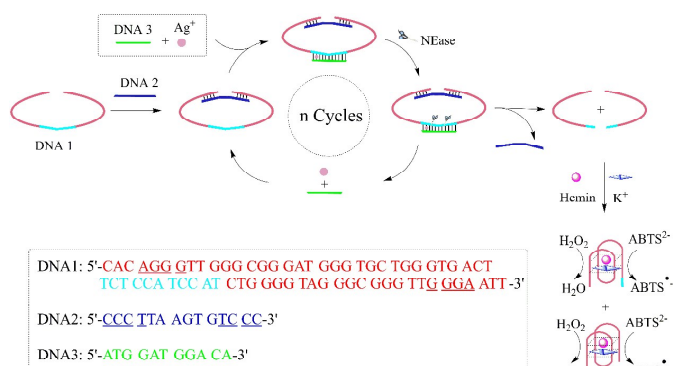
Scheme 1. Schematic illustration of the NEASA and G-quadruplex-based strategy for the detection of Ag+ and DNA oligonucleotides sequence used in this strategy.

The working principle of the designed NEASA and DNAzyme canalization based colorimetric biosensor is illustrated in Scheme 1. The system mainly consists of DNA1, DNA2, and DNA3. DNA1 includes two G-riched DNAzyme segments, the recognition sequence and cleavage site for nicking endonuclease (NEase), and the hybridization part for DNA2. DNA2 is designed to be partly complementary to both ends of DNA1. The DNA1/DNA2 duplex has the Tm of 40.6 °C (calculated using OligoAnalyzer 3.1 software from IDT, using 3 μM hybridization part of DNA1 (AGGGGGGA), and 1 μM Mg^{2+}), so it would be not very easily for the two strands to dissociate at 37 °C. DNA3 is designed to be complementary to DNA1 from 34th to 44th bases (5'-3') with one mismatched cytosine-cytosine. The hybridization of DNA1 and DNA2 results in DNA1 forming a closed structure. This closed structure holds the G-riched DNAzyme in a rigid stage, which cannot combine with hemin/K^+, which results in very low absorbance intensity (at 418 nm). Upon further addition of Ag^+, the complex of cytosine-Ag^+-cytosine forms and the hybridization of DNA1 and DNA3 can be achieved. The Tm of this part has a significant increase of more than 8 °C in the presence of Ag^+,[20] which ensures a low background in the following assay. The DNA1/DNA3 duplex has the Tm of 36.3 °C and 44.3 °C in the absence and presence of Ag^+, respectively (calculated using OligoAnalyzer 3.1 software from IDT, and obtained the Tm increase data from Ono's report[20]). Since the duplex DNA assisted by Ag^+ contains two endonuelease sites for Nt.CviPII, DNA1 can be cleaved into pieces by this NEase, which leads to the denaturation of the

DNA1/DNA2/DNA3 complex. Therefore, segments of DNA1 folds into G-quadruplexs, which is able to effectively catalyze the H_2O_2-mediated oxidation of $ABTS^{2-}$ in the presence of hemin, producing the free-radical ion $ABTS^{·-}$, which has a maximal absorption at 418 nm. Correspondingly, the reaction mixture produces a characteristic green color. Thus, the change in the absorption signal at 418 nm can be employed to monitor the formation of the G-quadruplex structure, which is closely related to Ag^+ concentration.

Feasibility Study
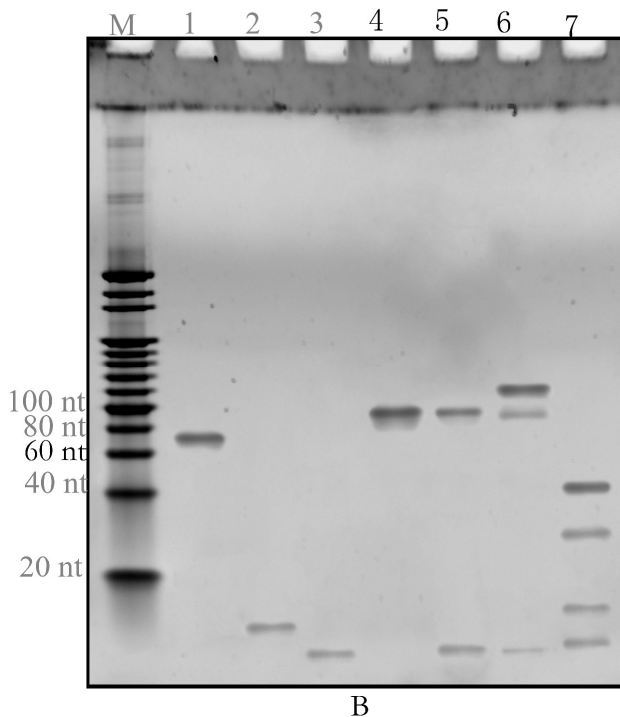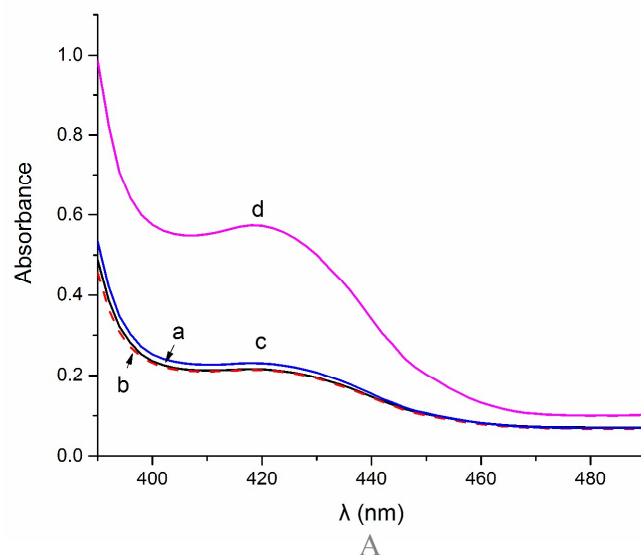
Fig. 1. (A) The UV-vis absorption intensity of the strategy under different conditions: (a) DNA1/DNA2/DNA3 with

NEase; (b) DNA1/DNA2/DNA3 without NEase; (c) 10 nM Ag^+ and DNA1/DNA2/DNA3, and (d) 10 nM Ag^+, DNA1/DNA2/DNA3, and NEase. (B) Nondenaturing polyacrylamide gel electrophoresis (PAGE) (20%) of the products by the amplification method. Lane (M): Marker. Lanes 1-7: (1) DNA1; (2) DNA2; (3) DNA3; (4) DNA1/DNA2 duplex; (5) DNA1/DNA2/DNA3 complex without Ag^+ (6) DNA1/DNA2/DNA3 complex with 100 nM Ag^+, and (7) DNA1/DNA2/DNA3 complex with 100 nM Ag^+ treated with NEase, respectively.

To verify the feasibility of the proposed assay strategy, the UV-vis absorption spectra under different conditions were investigated. As shown in Fig. 1A, the UV-vis absorbance intensity (at 418 nm) of the mixture of DNA1/DNA2/DNA3 with (curve a) and without (curve b) NEase was relatively low. After addition of 10 nM Ag^+ to the above mixture without NEase, the absorbance intensity at 418 nm increased was only 6.8% (curve c). However, when both 10 nM Ag^+ and NEase were present in the solution, we observed 165% of signal increase in the absorbance intensity at 418 nm (curve d). This demonstrated that the absorbance enhancement was attributed to the NEase activity. Thus, the proposed assay strategy could be used for amplified detection of Ag^+.

Gel Electrophoresis Characterization

The viability of proposed strategy was further investigated by gel electrophoresis. The results are shown in Fig. 1B. The lane numbered 1 shows the DNA1/DNA2 duplex, the lane numbered 2 shows the DNA1/DNA2/DNA3 complex with 100 nM Ag^+, and the lane numbered 3 shows DNA1/DNA2/DNA3 complex with 100 nM Ag^+ treated with NEase, respectively.

Sensitivity and Selectivity of the Ag^+ Sensing System
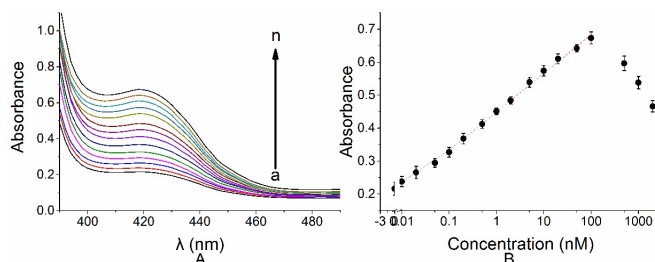
Fig. 2. (A) The UV-vis absorption intensity of the strategy for the assay of Ag^+ at different concentrations: from (a) to (n): 0, 0.01, 0.02, 0.05, 0.1, 0.2, 0.5, 1, 2, 5, 10, 20, 50, and 100 nM Ag^+, respectively. (B) The relationship between the absorption intensity and the logarithms of the concentrations of the Ag^+. The error bars represent relative standard deviations for three independent measurements.

To study the feasibility of this method for Ag^+ quantitation, the absorbance signal of the G-quadruplex solution as a function of Ag^+ concentration was measured. As shown in Fig. 2A, in the low Ag^+ concentration range, the signal increased with Ag^+ concentration and reached a maximum with 100 nM of Ag^+, indicating that the release of the quadruplex-forming oligomer is highly dependent on the concentration of Ag^+. When the concentration of Ag^+ exceeded 100 nM, the absorbance signal decreased dose-dependently with Ag^+, which may attribute to the Ag^+-mediated disruption of G-quadruplex

structures. Fig. 2B shows the corresponding calibration plot of the concentration of Ag^+ versus the UV-vis absorption intensity, in which the detection limit was calculated to be 0.01 nM according to the responses of the blank tests plus 3 times the standard deviation (3σ). The detection limit is not only more superior than previous reports, such as Miao's report (0.47 nM),[1] Kong's report (20 nM [11] and 50 nM,[4] but also much lower than the maximum level of silver in drinking water permitted by the United States Environmental Protection Agency (460 nM).[1] The fitting equation of the curve shown in Fig. 2B is $Y = 0.45 + 0.51 \times \ln (X + 0.0059)$ ($R^2 = 0.9979$), where Y is the absorption intensity and X is the concentration of Ag^+. These results demonstrated that the method has high sensitivity for the quantitative analysis of Ag^+.

The specificity detection
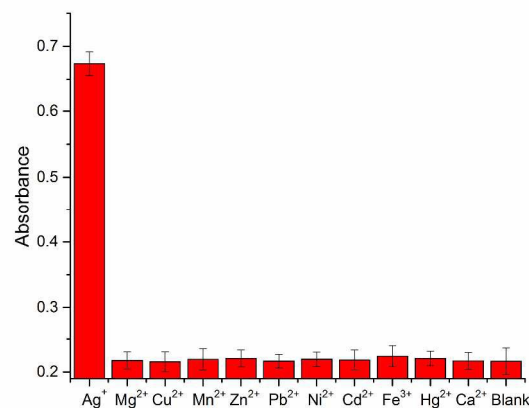
Fig. 3. Selectivity tests of this assay. The concentration of the ions are all 100 nM.

To test the specificity of the strategy, other metal ions were added to the sensor solution, and the absorbance in the presence of other ions were monitored. As shown in Fig. 3, none of the tested metal ions (Mg^{2+}, Cu^{2+}, Mn^{2+}, Zn^{2+}, Pb^{2+}, Ni^{2+}, Cd^{2+}, Fe^{3+}, Hg^{2+}, or Ca^{2+}) cause a detectable increase in absorbance. These results demonstrate that this approach exhibits excellent selectivity for Ag^+ detection over competing ions. Such high selectivity can be related to the highly specific binding capability of C–Ag^+–C base pairs. In other words, only the presence of Ag^+ can trigger amplification cycles to achieve enhanced visual detection of target.

Real samples analysis

Since Ag^+ may pose threats to the human health and environment, we have challenged this amplification strategy in drinking water and lake water to further prove its utility in real samples. Table 1 shows the experimental results obtained in real samples. The Ag^+ concentration recoveries of 93.0-109.4% were achieved. These results showed that the interference of drinking water and lake water could be overcome. This results indicated that this strategy has a promise in practical application with great accuracy and reliability for Ag^+ detection.

Table 1. Results of Ag$^+$ assay in real samples

Samples	Added (nM)	Detected (nM)	Recovery (%)	Relative error (%)
Drinking water	1	0.93	93.0	7.0
	20	21.38	106.9	6.9
Lake water	1	1.05	105.0	5.0
	20	21.88	109.4	9.4

Design of the Cys-Sensing System
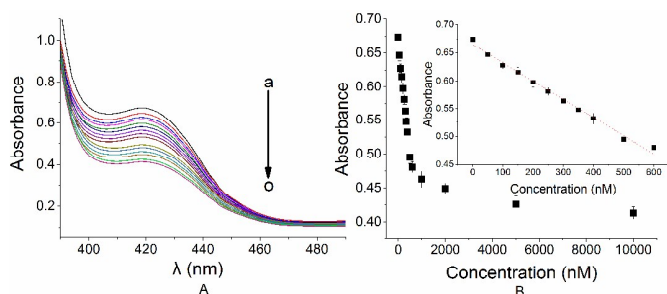
Fig. 4. (A) The UV-vis absorption intensity of the strategy for the assay of Cys at different concentrations: from (a) to (o): 0, 50,100, 150, 200, 250, 300, 350, 400, 500, 600, 1000, 2000, 5000, and 100000 nM Cys, respectively. (B) The relationship between the absorption intensity and the concentrations of the Cys. The inset shows the linear part ranging from 0 to 600 nM. The error bars represent relative standard deviations for three independent measurements.

Another sensing application of the strategy is to detection Cys. Cys interacts with Ag$^+$ and neutralizes its activity, so the Ag$^+$ detection method could be further explored as a Cys-detection method, based on competition between the DNA1/DNA3 and Cys, for binding to Ag$^+$. So, we have further conducted the studies on the assay of Cys. The concentration of Ag$^+$ is 100 nM, in view of the fact that the concentration of Ag$^+$ may give the maximum response at this concentration. As shown in Fig. 4A, the absorbance decreased with Cys concentration. When the concentration of Cys is further increased to 5000 nM, the Ag$^+$ will be fully inhibited (curve n). Fig. 4B shows the relationship between the UV-vis absorption and the concentration of Cys. A good linear range from 0 to 600 nM using an equation Y = 0.665 - 0.000328X (R^2 = 0.99), where Y is the absorption intensity and X is the concentration of Cys. A detection limit of 50 nM could be obtained according to the responses of the blank tests minus 3 times the standard deviation (3σ) (Fig. 4B insert).

Conclusions

In summary, we designed a highly sensitive and selective Ag$^+$-detection method by utilizing the advantages of both the nicking endonuclease-assisted signaling amplification (NEASA) strategy and the label-free architecture of G-quadruplex-hemin complex. The assay does not involve any chemical modification of DNA, which makes it simple and

low-cost. This "turn-on" process allowed the detection of Ag$^+$ at concentrations as low as 0.01 nM using a simple Uv-vis absorption technique. The technique was also explored as a Cys-sensing system by exploiting the competitive binding between C–Ag$^+$–C base pairs and Cys. Therefore, a simple visual method for Ag$^+$ or Cys detection might be developed from the technique described here.

Acknowledgements

Supplementary information

Electronic Supplementary Information (ESI) available:.See DOI: 10.1039/b000000x/

Notes and references

Key Laboratory of Nuclear Medicine, Ministry of Health, Jiangsu Key Laboratory of Molecular Nuclear Medicine, Jiangsu Institute of Nuclear Medicine. Wuxi, Jiangsu 214063, China. E-mail: zhangkai@jsinm.org (K Zhang)

1. P. Miao, L. Ning and X. Li, *Anal. Chem.*, 2013, **85**, 7966-7970.
2. M. Kumar, R. Kumar and V. Bhalla, *Org. Lett.*, 2010, **13**, 366-369.
3. C.-C. Chang, S. Lin, S.-C. Wei, Y. Chu-Su and C.-W. Lin, *Anal. Bioanal. Chem.*, 2012, **402**, 2827-2835.
4. X.-H. Zhou, D.-M. Kong and H.-X. Shen, *Anal. Chem.*, 2009, **82**, 789-793.
5. R.-H. Yang, W.-H. Chan, A. W. M. Lee, P.-F. Xia and H.-K. Zhang, *J. Am. Chem. Soc.*, 2003, **125**, 2884-2885.
6. A. Chatterjee, M. Santra, N. Won, S. Kim, J. K. Kim, S. B. Kim and K. H. Ahn, *J. Am. Chem. Soc.*, 2009, **131**, 2040-2041.
7. P. Miao, L. Ning and X. Li, *Anal. Chem.*, 2013, **85**, 7966-7970.
8. X. Zhu, J. Zhao, Y. Wu, Z. Shen and G. Li, *Anal. Chem.*, 2011, **83**, 4085-4089.
9. D. Huang, C. Niu, X. Wang, X. Lv and G. Zeng, *Anal. Chem.*, 2012, **85**, 1164-1170.
10. G. Mor-Piperberg, R. Tel-Vered, J. Elbaz and I. Willner, *J. Am. Chem. Soc.*, 2010, **132**, 6878-+.
11. D. M. Kong, L. L. Cai and H. X. Shen, *Analyst*, 2010, **135**, 1253-1258.
12. H.-M. Meng, T. Fu, X.-B. Zhang, N.-N. Wang, W. Tan, G.-L. Shen and R.-Q. Yu, *Anal. Chem.*, 2012, **84**, 2124-2128.
13. G. W. Collie and G. N. Parkinson, *Chem. Soc. Rev.*, 2011, **40**, 5867-5892.
14. R. Freeman, X. Liu and I. Winner, *J. Am. Chem. Soc.*, 2011, **133**, 11597-11604.
15. E. Golub, R. Freeman, A. Niazov and I. Willner, *Analyst*, 2011, **136**, 4397-4401.
16. K. Zhang, T. Ren, K. Wang, X. Zhu, H. Wu and M. Xie, *Chem. Commun.*, 2014, **50**, 13342-13345.
17. D. Koirala, C. Ghimire, C. Bohrer, Y. Sannohe, H. Sugiyama and H. Mao, *J. Am. Chem. Soc.*, 2013, **135**, 2235-2241.
18. G. Pelossof, R. Tel-Vered, X.-Q. Liu and I. Willner, *Chemistry-a European Journal*, 2011, **17**, 8904-8912.
19. K. Zhang, K. Wang, X. Zhu, J. Zhang, L. Xu, B. Huang and M. Xie, *Chem. Commun.*, 2014, **50**, 180-182.

20. A. Ono, S. Cao, H. Togashi, M. Tashiro, T. Fujimoto, T. Machinami, S. Oda, Y. Miyake, I. Okamoto and Y. Tanaka, *Chem. Commun.*, 2008, DOI: 10.1039/B808686A, 4825-4827.